Stem Cell Reports
Article

ISSCR

OPEN ACCESS

Promotion Effects of miR-375 on the Osteogenic Differentiation of Human Adipose-Derived Mesenchymal Stem Cells

Si Chen,[1] Yunfei Zheng,[2] Shan Zhang,[3] Lingfei Jia,[3,4,*] and Yongsheng Zhou[1,5,*]
[1]Department of Prosthodontics
[2]Department of Orthodontics
[3]Central Laboratory
[4]Department of Oral and Maxillofacial Surgery
[5]National Engineering Lab for Digital and Material Technology of Stomatology, Beijing Key Laboratory of Digital Stomatology
Peking University School and Hospital of Stomatology, 22 Zhongguancun South Avenue, Haidian District, Beijing 100081, China
*Correspondence: jialingfei1984@sina.com (L.J.), kqzhouysh@hsc.pku.edu.cn (Y.Z.)
http://dx.doi.org/10.1016/j.stemcr.2017.01.028

SUMMARY

MicroRNA plays an important role in bone tissue engineering; however, its role and function in osteogenic differentiation warrant further investigation. In this study, we demonstrated that miR-375 was upregulated during the osteogenic differentiation of human adipose-derived mesenchymal stem cells (hASCs). Overexpression of miR-375 significantly enhanced hASCs osteogenesis both in vitro and in vivo, while knockdown of miR-375 inhibited the osteogenic differentiation of hASCs. Mechanistically, microarray analysis revealed *DEPTOR* as a target of miR-375 in hASCs. Knockdown of *DEPTOR* accelerated the osteogenic differentiation of hASCs by inhibiting AKT signaling, which mimics miR-375 overexpression. Furthermore, we confirmed that miR-375 regulated osteogenesis by targeting *YAP1*, and that YAP1 reversely bound to miR-375 promoter to inhibit miR-375 expression. Taken together, our results suggested that miR-375 promoted the osteogenic differentiation of hASCs via the YAP1/DEPTOR/AKT regulatory network, indicating that miR-375-targeted therapy might be a valuable approach to promote bone regeneration.

INTRODUCTION

Tissue engineering technology has become one of the most prospective therapeutic approaches for bone regeneration in bone defects (Guan et al., 2012; Petite et al., 2000). As a type of adult mesenchymal stem cells (MSCs), human adipose-derived mesenchymal stem cells (hASCs) are capable of self-renewal and differentiation into cells such as osteoblasts, chondrocytes, and adipocytes (Zuk et al., 2002). Because they can be obtained from adipose tissue in abundance by means of a minimally invasive procedure, hASCs are a valuable source of adult MSCs for bone tissue engineering and bone regeneration (Bosnakovski et al., 2005). Therefore, how to effectively promote the osteogenic differentiation of hASCs has become dramatically important in bone tissue engineering.

MicroRNAs (miRNAs) are a class of endogenously small non-coding RNAs that function as post-transcriptional regulators through binding to complementary sites on target mRNAs (Ha and Kim, 2014). Evolutionary conserved, miRNAs have been implicated in various biological processes, including the cell fate of embryonic stem cells, cell proliferation, apoptosis, differentiation, and carcinogenesis (Fang et al., 2015; Farazi et al., 2013; Hilton et al., 2013). A number of miRNAs participate in the osteogenic differentiation of MSCs, such as miR-21 (Sun et al., 2015), miR-31 (Deng et al., 2013), miR-34a (Fan et al., 2016), and miR-196a (Kim et al., 2009). Targeting miRNAs as a therapeutic approach has shed light on bone tissue regeneration, but the mechanism of their regulation of osteogenesis in MSCs remains to be determined (Zhang et al., 2016).

microRNA-375 (miR-375) was identified early as a pancreatic islet-specific miRNA regulating insulin secretion (Poy et al., 2004). Subsequent studies revealed that miR-375 participated in multiple biological processes, including glucose homeostasis, mucosal immunity, and cancer development (Biton et al., 2011; EI Ouaamari et al., 2008; Yan et al., 2014). Moreover, miR-375 is significantly downregulated in several types of tumors, and suppresses their proliferation by targeting some important genes, e.g., *JAK2*, *YAP1*, and *PDK1* (Ding et al., 2010; Zhang et al., 2013; Zhou et al., 2014). Research has shown that miR-375 is a negative regulator of adipogenic differentiation by targeting bone morphogenetic protein receptor 2 (BMPR2) (Liu et al., 2016a). Osteoblastic and adipocytic lineages have alternative fates during development and aging, and increased adipogenesis correlates with decreased osteogenesis (Takada et al., 2009; Verma et al., 2002), which led us to speculate that miR-375 might play a role in the differentiation of stem cells toward osteogenic lineage.

Osteogenic differentiation is a complex process governed by interplay of several signaling pathways (Novack, 2011; Salazar et al., 2016). Phosphatidylinositol 3-kinase (PI3K)/AKT/mammalian target of rapamycin (mTOR) and Hippo are two major pathways involved in the regulation of cell proliferation and differentiation (Hansen et al., 2015a; Laplante and Sabatini, 2012). Crosstalk between the two pathways plays a significant role in regulating

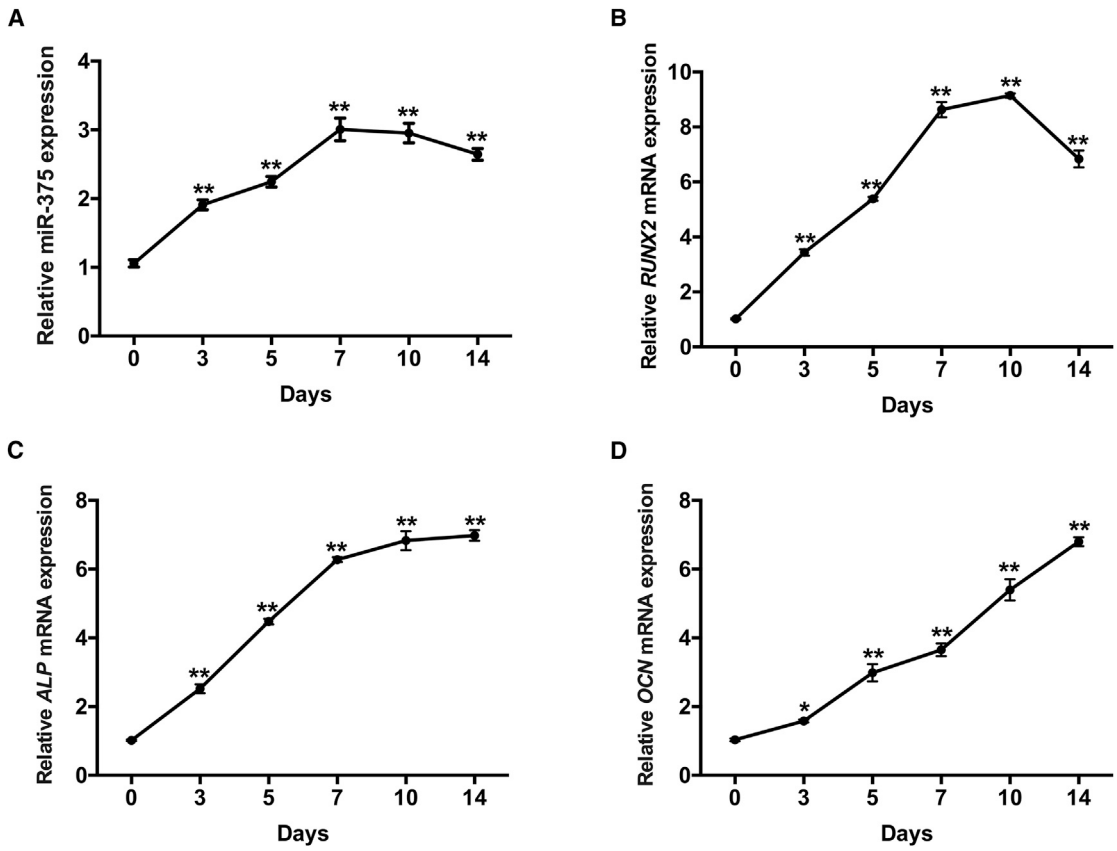

Figure 1. miR-375 Is Upregulated during the Osteogenic Differentiation of hASCs

(A) Relative expression of miR-375 at various time points during the osteogenic differentiation of hASCs as determined by qRT-PCR. U6 was used for normalization.

(B–D) Relative mRNA levels of the osteogenic markers *RUNX2*, *ALP*, and *OCN* at various time points during the osteogenic differentiation of hASCs as determined by qRT-PCR. *GAPDH* was used for normalization.

Data are presented as mean ± SD. *p < 0.05, **p < 0.01 (n = 3 independent experiments).

cell proliferation and differentiation (Hansen et al., 2015b; Shimobayashi and Hall, 2014). The PI3K/AKT/mTOR pathway governs a variety of cellular and molecular responses by regulating protein synthesis (Dibble and Cantley, 2015). Perturbation of this pathway contributes to the maintenance of bone homeostasis and MSC lineage differentiation (Martin et al., 2015). The Hippo pathway plays a crucial role in organ-size control by modulating cell proliferation and apoptosis (Zhao et al., 2011). Yes-associated protein 1 (YAP1), major downstream effector of the Hippo pathway, inhibits the osteogenic differentiation of bone marrow-derived MSCs (BMSCs) (Sen et al., 2015; Seo et al., 2013). In this study, we evaluated the effects of miR-375 in hASC osteogenesis and demonstrated that miR-375 promoted the osteogenic differentiation of hASCs via a YAP1/DEPTOR/AKT regulatory network, suggesting its potential utility in hASC-based bone tissue engineering.

RESULTS

miR-375 Is Upregulated during the Osteogenic Differentiation of hASCs

The expression of miR-375 was determined by qRT-PCR at various time points during hASC osteogenesis. The result showed that miR-375 expression was upregulated after induction to the osteogenic lineage and remained at a high level during osteogenesis (Figure 1A). Moreover, the expression levels of osteogenic markers *RUNX2*, alkaline phosphatase (*ALP*), and osteocalcin (*OCN*) were also upregulated during the osteogenic differentiation (Figures 1B–1D).

miR-375 Promotes the Osteogenic Differentiation of hASCs In Vitro

Lentivirus was used to overexpress or knock down miR-375 in hASCs. The transduction efficiency was estimated to be

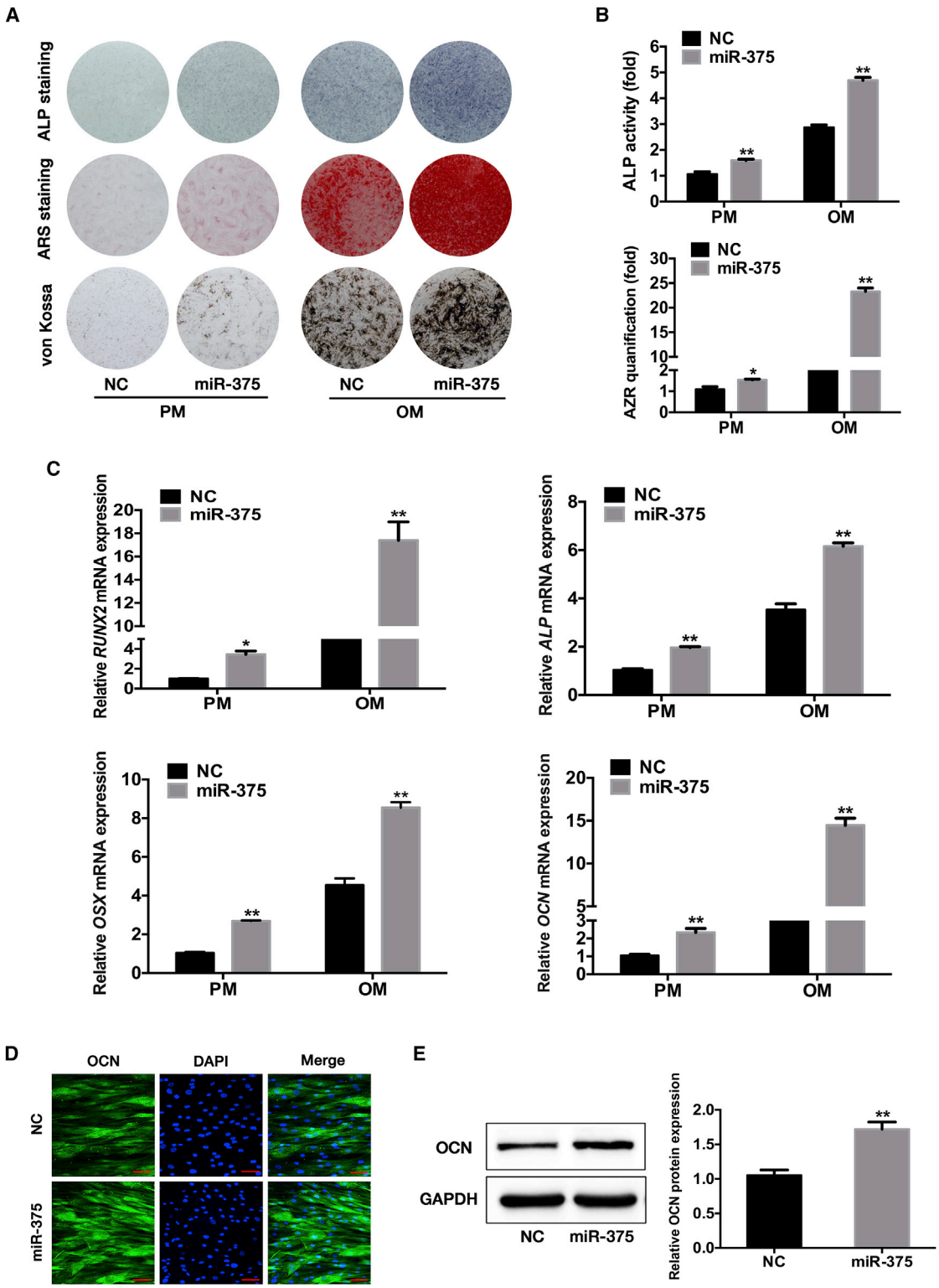

Figure 2. miR-375 Overexpression Promotes the Osteogenic Differentiation of hASCs

hASCs were transfected with lentivirus expressing miR-375 or control vector (NC), and cultured in proliferation medium (PM) or osteogenic medium (OM).

(legend continued on next page)

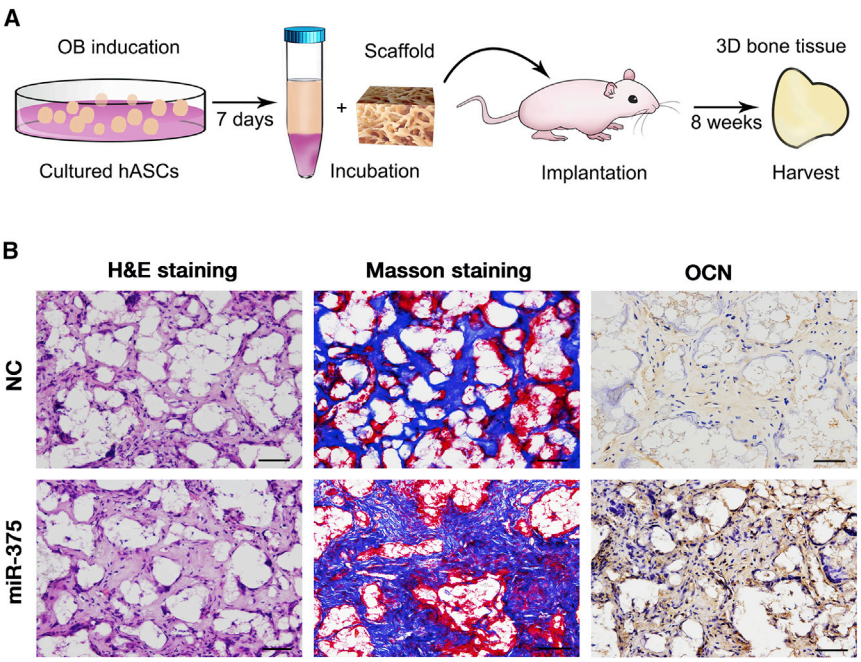

Figure 3. miR-375 Overexpression Promotes Heterotopic Bone Formation In Vivo

(A) Schematic of the experimental setup.

(B) H&E staining, Masson's trichrome staining, and immunohistochemical staining of OCN in miR-375 and NC groups. Scale bars, 50 μm.

See also Figure S3.

more than 80%, as evaluated by the percentage of GFP-positive cells 72 hr after transduction (Figure S1A). qRT-PCR analysis of miR-375 expression confirmed an almost 100-fold increase in the miR-375 overexpression group (miR-375) and a ~70% decrease in the miR-375 knockdown group (anti-miR-375) compared with the control group (negative control [NC] or anti-NC) (Figure S1B). ALP staining and quantification showed that overexpression of miR-375 enhanced the osteogenic differentiation of hASCs cultured in proliferation medium (PM) or osteogenic medium (OM) on day 7 (Figures 2A and 2B), while miR-375 knockdown inhibited the ALP activity (Figures S2A and S2B). The extracellular mineralization of hASCs, as measured by alizarin red S (ARS) and von Kossa (VK) staining in PM or OM on days 14 and 21, respectively, displayed outcomes similar to those of ALP assays (Figures 2A, 2B, S2A, and S2B). Consistently, overexpression of miR-375 significantly increased the expression of osteogenesis-associated genes, including *RUNX2*, *ALP*, osterix (*OSX*), and *OCN* (Figure 2C), while miR-375 knockdown showed the opposite tendency (Figure S2C). Moreover, immunofluorescence staining and western blotting indicated that the protein level of OCN was increased in the miR-375 overexpression group (Figures 2D and 2E) and reduced in the miR-375 knockdown group (Figures S2D and S2E).

miR-375 Promotes the Osteogenic Differentiation of hASCs In Vivo

hASCs expressing miR-375 and NC were loaded onto scaffolds and implanted in the subcutaneous space of nude mice (six mice per group) (Figure 3A). After 8 weeks, the implantation samples were harvested and subjected to computed microtomography (micro-CT) imaging. Representative images showed that the miR-375 overexpression group exhibited more newly formed bone with fewer scaffold remnants compared with the NC group (Figure S3A). Moreover, the percentages of bone volume to tissue volume (BV/TV) ratio in the miR-375 overexpression group was almost three times higher than that in the NC group, and the percentage of bone surface to tissue volume (BS/TV)

(A) Alkaline phosphatase (ALP) staining on day 7, alizarin red S (ARS) staining on day 14, and von Kossa (VK) staining on day 21 after osteogenic induction.

(B) ALP activity on day 7 and ARS mineralization assay on day 14 after osteogenic induction.

(C) Relative mRNA levels of *RUNX2* and *ALP* measured by qRT-PCR on day 7 of osteogenic induction. Relative mRNA levels of *OSX* and *OCN* measured by qRT-PCR on day 14 of osteogenic induction. *GAPDH* was used for normalization.

(D) Confocal microscopy of OCN with DAPI counterstaining on day 14 after osteogenic induction. Scale bars, 200 μm.

(E) Left: western blot of OCN protein level on day 14 after osteogenic induction. GAPDH was used as the internal control. Right: quantification of band intensities.

Data are presented as mean ± SD. *$p < 0.05$, **$p < 0.01$ ($n = 3$ independent experiments). See also Figures S1 and S2.

ratio in the miR-375 overexpression group was lower than that in the NC group (Figure S3B). H&E staining revealed little newly formed bone in the NC group, while osteoid was formed in the miR-375 overexpression group. Collagen organization with blue color in Masson's trichrome staining was significantly higher in the miR-375 overexpression group. Furthermore, immunohistochemical staining for OCN indicated that both the range and intensity of the stained granules in osteoblasts were generally increased in the miR-375 overexpression group (Figure 3B).

miR-375 Inhibits *DEPTOR* by Targeting Its 3′ UTR

To evaluate the molecular mechanisms by which miR-375 regulates osteogenic differentiation, we established miR-375-overexpressing hASCs and conducted a transcriptome microarray analysis 7 days after osteoinduction. A scatterplot showed overexpression of miR-375 resulting in upregulation of 106 genes and downregulation of 91 (Figure 4A). Pathway analysis reveals that miR-375 is involved in the organization of extracellular matrix, and several signaling pathways, such as nuclear factor κB, PI3K-AKT, and mitogen-activated protein, are enriched in this process (Figure 4B). Among the downregulated genes, *DEPTOR* was distinguished by a particularly marked decrease (Table S1). qRT-PCR and western blot analysis confirmed that DEPTOR expression was decreased in miR-375-overexpressing hASCs compared with control cells (Figures 4C and 4D). We next assessed the putative binding site of miR-375 in the 3′ UTR of *DEPTOR* using RNA22 prediction software (Figure 4E). Luciferase activity analysis showed that miR-375 repressed the luciferase expression of vectors containing the 3′ UTR of wild-type *DEPTOR* (*DEP*-WT), but had no effect on the mutant-type *DEPTOR* (*DEP*-MT) (Figure 4F).

Knockdown of *DEPTOR* Promotes the Osteogenic Differentiation of hASCs

To investigate the role of *DEPTOR* in hASCs osteogenesis, we determined its expression by qRT-PCR at various time points after induction to the osteogenic lineage. The result showed that *DEPTOR* expression was dramatically downregulated and remained at a low level during the osteogenic differentiation of hASCs (Figure 5A), which is a tendency opposite to that of miR-375 expression (Figure 5B). Two *DEPTOR* small interfering RNA (siRNA) sequences were designed to knock down *DEPTOR* in hASCs, and the knockdown efficiency was ~30% as determined by qRT-PCR and western blot (Figures 5C and 5D). Moreover, ALP staining and quantification showed that knockdown of *DEPTOR* accelerated the osteogenic differentiation of hASCs cultured in PM or OM on day 7 (Figures 5E and 5F). The extracellular matrix mineralization, as measured by ARS staining and quantification on day 14, was also increased in *DEPTOR* siRNA-treated cells (Figures 5E and 5F). Moreover, expression of RUNX2 and OCN at both mRNA and protein levels was significantly elevated in *DEPTOR* knockdown groups (Figures 5G and 5H).

miR-375 Inhibits AKT Signaling by Directly Targeting *DEPTOR*

Since DEPTOR has been reported as an endogenous mTOR inhibitor (Peterson et al., 2009), we further examined mTOR complex 1 (mTORC1) and mTORC2 pathway status in *DEPTOR* knockdown hASCs. The phosphorylated form of S6K (Thr389), a downstream effector of mTORC1, increased in *DEPTOR* knockdown groups (Figures 6A and 6B), indicating activation of mTORC1. In contrast, the level of phospho-mTOR at Ser2448 was downregulated in *DEPTOR* knockdown groups (Figures 6A and 6B). Knockdown of *DEPTOR* led to suppression of the phosphorylated form of AKT (Ser473), indicating suppression of mTORC2 (Figures 6A and 6B). Moreover, knockdown of *DEPTOR* resulted in downregulation of the phospho-IRS1 (Ser636/639) level (Figures 6A and 6B). This regulation suggested a strong feedback inhibition of the IRS1-PI3K-AKT pathway by S6K. IRS1 contains several PI3K binding domains, which are responsible for the activation of PI3K and AKT. S6K phosphorylates IRS1 to prevent its binding to PI3K (Laplante and Sabatini, 2012; Srinivas et al., 2016). To ascertain whether miR-375 inhibited AKT signaling by directly targeting *DEPTOR*, we detected AKT signaling status in miR-375 overexpression hASCs. The results showed that overexpression of miR-375 had similar effects to those of *DEPTOR* knockdown in terms of AKT signaling (Figures 6C and 6D).

Direct Targeting of *YAP1* by miR-375

As a transcriptional regulator, *YAP1* transcript contains a conserved miR-375 targeting site in its 3′ UTR (Liu et al., 2010; Zhang et al., 2013). Thus, we constructed luciferase reporter plasmids containing the wild-type or mutant-type miR-375 target site in the *YAP1* 3′ UTR sequence (Figure S4A). miR-375 repressed the luciferase expression of vectors containing the 3′ UTR of wild-type *YAP1* (*YAP1*-WT), but had no effect on the mutant-type *YAP1* (*YAP1*-MT) (Figure S4B). Overexpression of miR-375 led to downregulation of YAP1 at both mRNA and protein levels (Figure S4C), indicating that miR-375 negatively regulates *YAP1* by binding directly to the 3′ UTR of its mRNA. Furthermore, we examined *YAP1* expression during the osteogenic differentiation of hASCs, and qRT-PCR showed that the expression of *YAP1* was decreased during osteogenic differentiation (Figure S4D).

miR-375 and YAP1 Form a Negative Feedback Loop

As a transcriptional factor, YAP1 plays a crucial role in the biogenesis of miRNAs (Mori et al., 2014), we determined

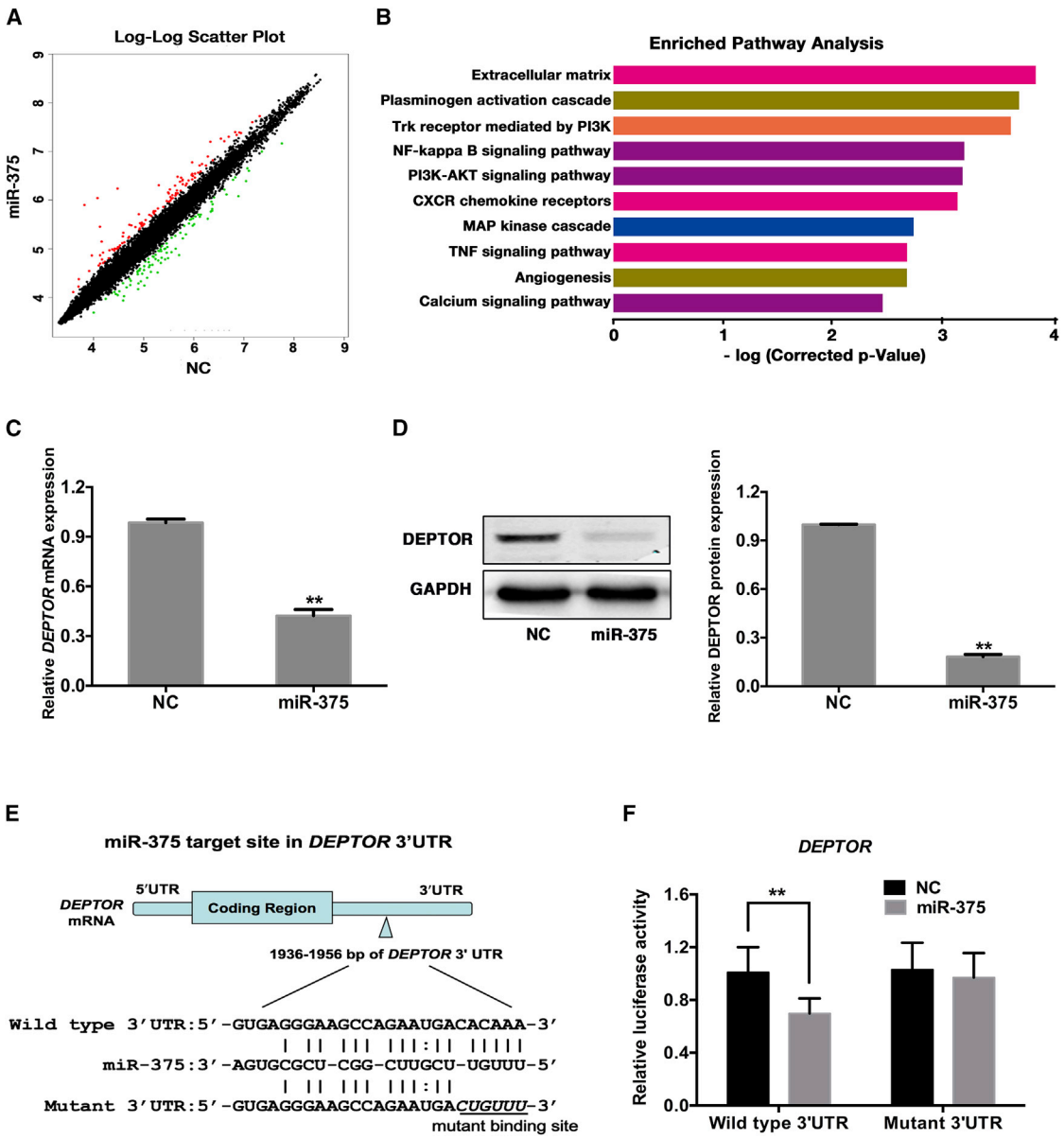

Figure 4. miR-375 Overexpression Inhibits *DEPTOR* by Targeting Its 3′ UTR

hASCs were transfected with lentivirus expressing miR-375 or control vector (NC).

(A) 106 genes (red block) were upregulated and 91 (green block) were downregulated in miR-375-overexpressing hASCs 7 days after osteoinduction. A change $\geq$1.5 indicates upregulation and $\leq$0.667 indicates downregulation.

(B) Enriched pathway analysis with miR-375 overexpression in hASCs 7 days after osteogenic induction.

(C) Relative mRNA expression of *DEPTOR* measured by qRT-PCR in miR-375 and NC groups. *GAPDH* was used for normalization.

(D) Left: western blot of DEPTOR protein levels in miR-375 and NC groups. GAPDH was used as the internal control. Right: quantification of band intensities.

(E) Predicted binding site of miR-375 in the 3′ UTR of *DEPTOR*-WT mRNA (mutated bases in the 3′ UTR of *DEPTOR*-MT are underlined).

(F) Luciferase activity of cells with miR-375 overexpression in *DEPTOR*-WT and *DEPTOR*-MT groups.

Data are presented as mean ± SD. **p < 0.01 (n = 3 independent experiments). See also Table S1.

whether YAP1 regulates the transcription of miR-375. Two *YAP1* siRNA sequences were designed to knock down *YAP1* in hASCs, and both markedly decreased YAP1 expression (Figure 7A). qRT-PCR indicated that miR-375 expression was upregulated in *YAP1* knock-down groups (Figure 7B). We next investigated whether

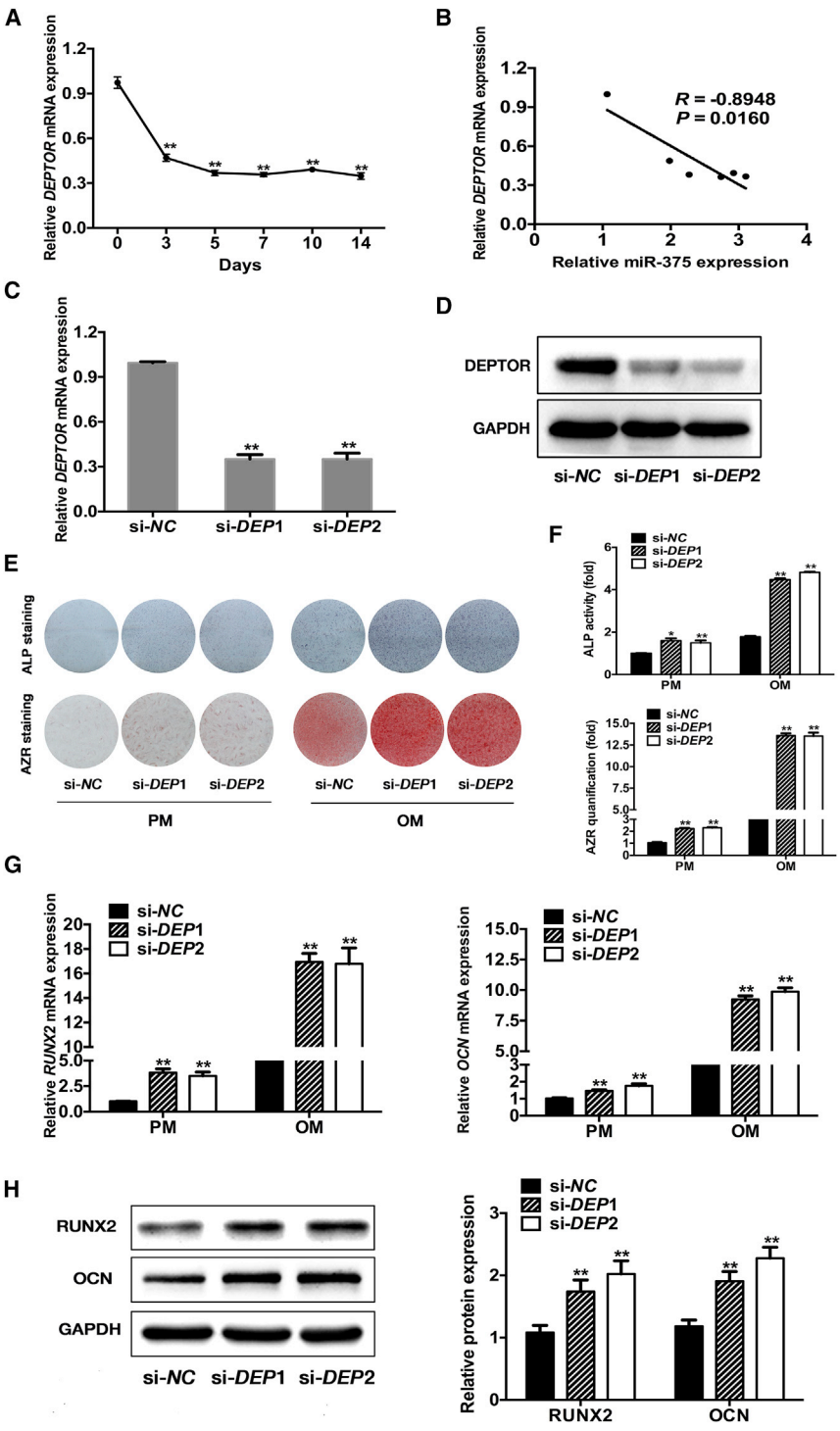

Figure 5. *DEPTOR* Knockdown Promotes the Osteogenic Differentiation of hASCs

(A) Relative expression of *DEPTOR* at various time points during the osteogenic differentiation of hASCs as determined by qRT-PCR. *GAPDH* was used for normalization.

(B) *DEPTOR* expression is negatively correlated with that of miR-375 during the osteogenic differentiation of hASCs. *DEPTOR* and miR-375 expression was determined by qRT-PCR; *DEPTOR* expression was normalized to that of *GAPDH*, whereas miR-375 was normalized to U6. p and R values were calculated using Spearman's correlation tests.

(C) Relative mRNA levels of *DEPTOR* at 48 hr after transfection of hASCs with *DEPTOR* siRNA (si-*DEP*1, si-*DEP*2) or the control vector (si-*NC*). *GAPDH* was used for normalization.

(D) Western blot of DEPTOR protein levels 48 hr after transfection of hASCs with *DEPTOR* siRNA or control vector. GAPDH was used as the internal control.

(E–H) hASCs were transfected with *DEPTOR* siRNA or control vector and cultured in PM or OM. (E) Alkaline phosphatase (ALP) staining on day 7 and alizarin red S (ARS) staining on day 14 after osteogenic induction. (F) ALP activity on day 7 and ARS mineralization assay on day 14 after osteogenic induction. (G) Relative mRNA levels of *RUNX2* and *OCN* measured by qRT-PCR on day 14 after osteogenic induction. *GAPDH* was used for normalization. (H) Left: western blot of RUNX2 and OCN protein levels on day 14 after osteogenic induction. GAPDH was used as the internal control. Right: quantification of band intensities.

Data are presented as mean ± SD. *p < 0.05, **p < 0.01 (n = 3 independent experiments).

YAP1 is directly responsible for miR-375 transcription. A sequence analysis of the promoter region of miR-375 −4,000 bp upstream of the transcription start site revealed putative binding sites for TEAD, a transcription factor that mediates the function of YAP1 (Zhao et al., 2011). A chromatin immunoprecipitation (ChIP) assay was performed using an antibody against YAP1 and five pairs of primers flanking the region of the predicted YAP1 binding sites on the miR-375 promoter (Figure 7C). The result showed that knockdown of *YAP1* dramatically

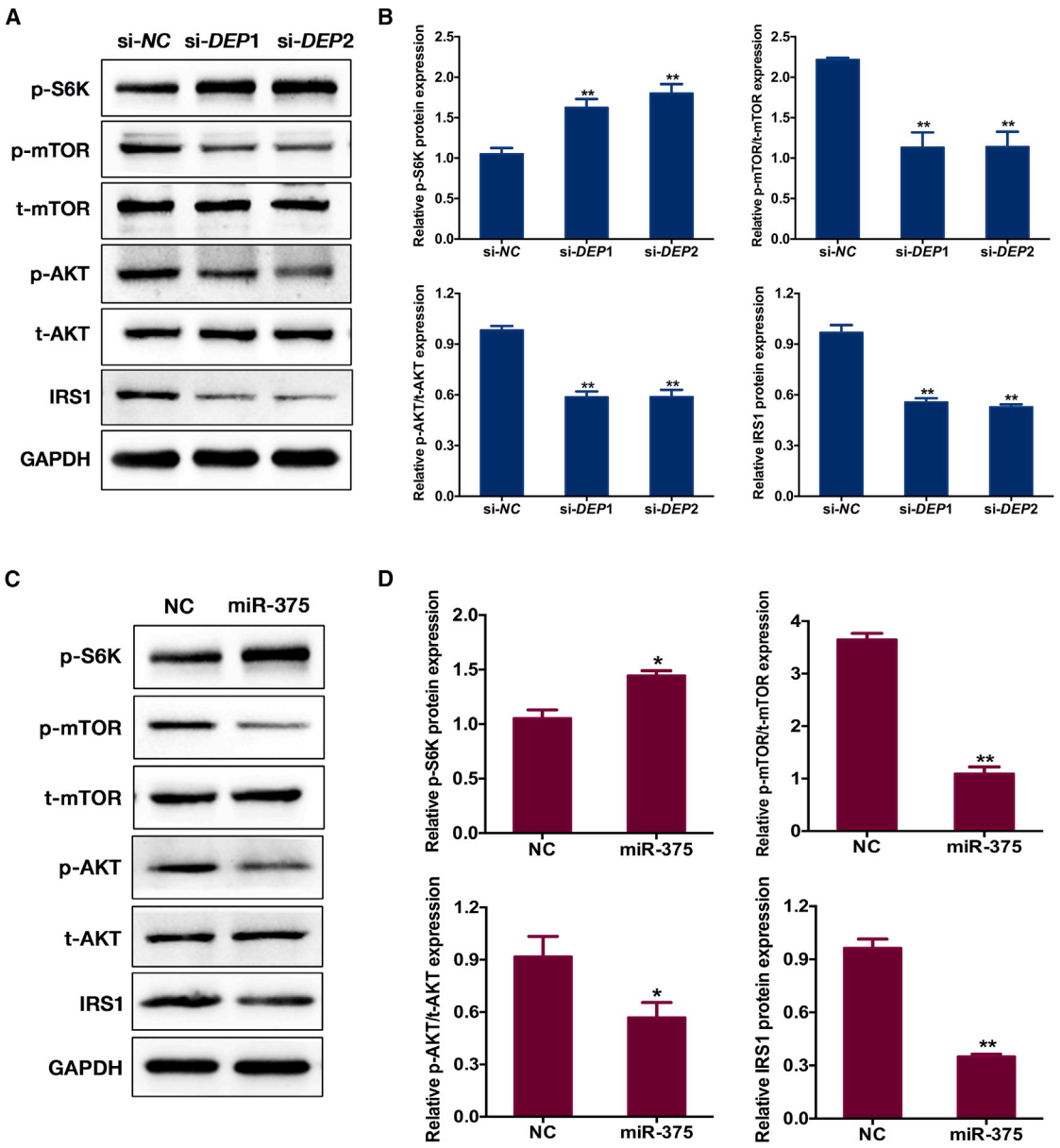

Figure 6. miR-375 Inhibits AKT Signaling by Directly Targeting *DEPTOR*

(A and B) Knockdown of *DEPTOR* inhibited AKT signaling through feedback inhibition of S6K-IRS1-AKT pathway in hASCs, which was evidenced by upregulation of p-S6K (Thr389), downregulation of p-mTOR (Ser2448), inhibition of p-AKT (Ser473), and p-IRS1 (Ser636/639). GAPDH was used as the internal control. Bar graphs (B) show the quantification of band intensities.

(C and D) Expression analysis of AKT signaling with miR-375 overexpression in hASCs. Protein levels of p-S6K (Thr389), p-mTOR (Ser2448), t-mTOR, p-AKT (Ser473), t-AKT, and p-IRS1 (Ser636/639) were determined by western bolt analysis. GAPDH was used as the internal control. Bar graphs (D) show the quantification of band intensities.

Data are presented as mean ± SD. *$p < 0.05$, **$p < 0.01$ ($n = 3$ independent experiments).

decreased the levels of *YAP1* in the fragment containing Ch-3 and Ch-4 (Figure 7D), suggesting that the distal −3,000 bp to −1,000 bp region contains a TEAD-response element. Moreover, we transfected a luciferase reporter containing the wild-type or mutant miR-375 promoter in *YAP1* knockdown cells (Figure 7E), and knockdown of *YAP1* dramatically increased the luciferase expression in cells transfected with the wild-type miR-375 promoter but not with the mutant reporter (Figure 7F).

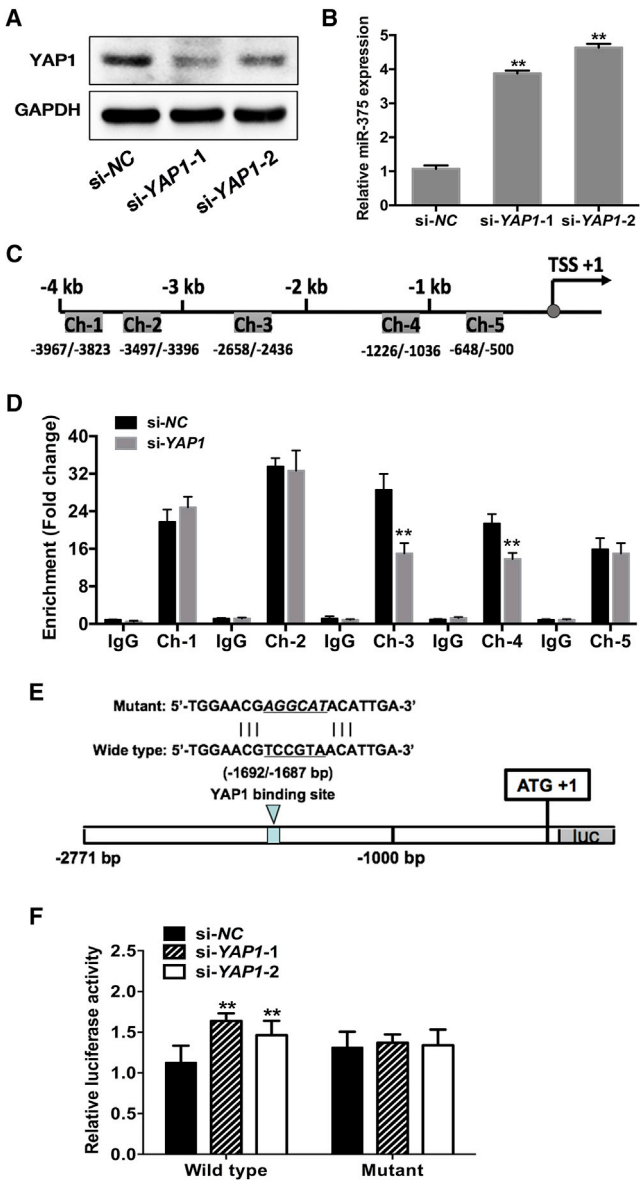

Figure 7. YAP1 Negatively Regulates miR-375 by Binding to Its Promoter

hASCs were transfected with *YAP1* siRNA (si-*YAP1*-1, si-*YAP1*-2) or the control vector (si-NC).

(A) Western blot of YAP1 protein levels in the si-*YAP1*-1, si-*YAP1*-2, and si-*NC* groups. GAPDH was used as the internal control.

(B) Relative expression of miR-375 in the si-*YAP1*-1, si-*YAP1*-2, and si-*NC* groups as determined by qRT-PCR. U6 was used for normalization.

(C) Diagram of the miR-375 promoter and location of the primers. The positions marked are relative to the transcription start site (TSS).

(D) ChIP-qPCR showing the interaction between the YAP1 and the miR-375 promoter in hASCs in the si-*YAP1*-1 and si-*NC* groups. IgG was used for normalization.

(E) The YAP1 binding site on the miR-375 promoter (bottom) and mutation of YAP1 binding site (top).

(F) Knockdown of *YAP1* increased the luciferase reporter activity of the wild-type, but not the mutant miR-375 promoter.

Data are presented as mean ± SD. **p < 0.01 (n = 3 independent experiments). See also Figures S4 and S5.

Knockdown of *YAP1* Enhanced the Osteogenic Differentiation of hASCs

ALP staining and quantification indicated that knockdown of *YAP1* promoted the osteogenic differentiation of hASCs cultured in PM or OM on day 7 (Figures S5A and S5B). The extracellular matrix mineralization, as measured by ARS staining and quantification on day 14, was also increased in *YAP1* siRNA-treated cells (Figures S5A and S5B). Moreover, expression levels of the osteogenesis-related genes *RUNX2* and *OCN* were elevated in *YAP1* knockdown groups (Figure S5C).

DISCUSSION

miR-375 has been implicated in various biological processes, but its role and function in osteogenic differentiation require further investigation. In this study, we found that miR-375 was unregulated during the osteogenic differentiation of hASCs, and overexpression of miR-375 promoted hASCs osteogenesis both in vitro and in vivo. This is inconsistent with a previous report, which indicated that miR-375 exerted a negative regulatory effect on the osteogenic differentiation of C2C12 cells (Du et al., 2015). This difference might be attributed to cell lines utilized in the two studies. C2C12 cells were isolated from mouse myoblasts and did not have multiple differentiation potential, while hASCs used in this study were derived from human adipose tissue and capable of multi-lineage differentiation (Zuk et al., 2002). Moreover, to elucidate whether miR-375 promotes osteogenesis of MSCs from other sources, we overexpressed miR-375 in BMSCs, the results of which showed that overexpression of miR-375 also promoted the osteogenic differentiation of BMSCs (our unpublished data).

To unveil the underlying molecular mechanisms by which miR-375 promotes hASC osteogenesis, we conducted a microarray analysis 7 days after osteoinduction. According to the microarray profiles, the osteogenesis-associated genes *RUNX2* (ratio = 1.6431) and *ALP* (ratio = 1.6367) were upregulated, and *DEPTOR* expression was decreased. As an mTOR-interacting protein, DEPTOR endogenously inhibits the activity of mTOR (Peterson et al., 2009). Furthermore, DEPTOR plays a key role in maintaining the pluripotency of embryonic stem cells (ESCs) (Agrawal et al., 2014). Recent studies demonstrated that DEPTOR was a crucial regulator of adipogenic differentiation, and that its overexpression and suppression

promote and block adipogenesis, respectively (Caron et al., 2016; Laplante et al., 2012). Here, we showed that *DEPTOR* is downregulated during the osteogenic differentiation of hASCs and that its knockdown resulted in enhanced mineralization activity of hASCs and elevated expression of osteogenesis-associated markers. Promotion effects of miR-375 on the osteogenic differentiation of hASCs might be attributed to repression of *DEPTOR*, which leads to loss of stem cell pluripotency.

The Hippo pathway is now being recognized as an integrator of mechanical and cellular-contact-dependent sensory signals with the intracellular components that regulate cell fate (Yang et al., 2014). Active Hippo signaling inhibits the transcriptional activity of YAP1 and TAZ by phosphorylating and sequestering them in the cytoplasm (Meng et al., 2016). Although YAP1 and TAZ are often considered functionally analogous orthologs of *Drosophila* Yorkie (Yki), their functions in osteogenic differentiation remains distinct. TAZ was identified as a fate-determination factor that binds to and activates RUNX2, a transcriptional regulator of the osteoblast lineage, while YAP1 was downregulated during the osteogenic differentiation of MSCs and suppressed their osteogenesis by binding to β-catenin to inhibit WNT signaling (Hong et al., 2005; Seo et al., 2013). Several studies have shown that *YAP1* contains an miR-375 target site in its 3′ UTR and represses tumorigenesis in carcinomas (Liu et al., 2010; Selth et al., 2016). In our study, miR-375 directly targeted the predicted binding site of *YAP1*, resulting in its downregulation during the osteogenic differentiation of hASCs.

YAP1 maintains the pluripotency of ESCs by binding to a number of "stemness" genes, including Nanog, OCT4, and SOX2 (Lian et al., 2010), and often acts as a transcriptional co-activator (Hong and Guan, 2012). In some instances, YAP1 also functions as a transcriptional co-repressor (Kim et al., 2015). Moreover, studies focused on miRNA biogenesis reveal that activation of YAP1 is responsible for the widespread miRNA repression. The mechanism might lie in DEAD box helicase 17 (DDX17), a microprocessor component. Knockdown of *YAP1* facilitates DDX17 association with microprocessor and binding to a specific sequence motif in pri-miRNA (Mori et al., 2014). However, YAP1 conversely induces the biogenesis of some miRNAs, such as miR-16, -21, and -23, by increasing Dicer through the Let-7 family (Chaulk et al., 2014). In our study, we show that knockdown of *YAP1* in hASCs increased miR-375 expression by binding to its promoter. The upregulation of miR-375 during the osteogenic differentiation of hASCs was modulated, at least in part, by the decrease in YAP1 expression.

As a nutrient sensor, mTOR responds to PI3K-mediated growth factor signaling to regulate cell growth in mammals (Dibble and Cantley, 2015). The PI3K/AKT/mTOR pathway is involved in osteogenic differentiation and osteoporosis (Martin et al., 2010; Xi et al., 2015). Here, we demonstrated that miR-375 overexpression activated S6K via mTORC1, leading to a negative feedback inhibition of IRS1-PI3K-AKT in hASCs, resulting in a decrease in the phosphorylated AKT level. Moreover, YAP1 inhibits the transcription of PTEN and then activates PI3K/AKT/mTOR signaling by inducing miR-29 (Tumaneng et al., 2012). As a key downstream effector of the Hippo pathway, YAP1 plays a crucial role in regulating cell proliferation and organ size (Hansen et al., 2015a). Our research indicated that knockdown of *YAP1* induced the transcription of miR-375, thus activating AKT signaling by directly targeting *DEPTOR*. The link from YAP1 to miR-375 to DEPTOR and AKT suggests their collaboration in cell growth control, and illustrates that signaling networks function in a coordinated manner to fine-tune the osteogenic differentiation of MSCs.

In summary, our findings indicated that miR-375 promoted the osteogenic differentiation of hASCs both in vitro and in vivo, and miR-375 targeted *DEPTOR* to inhibit the activity of AKT signaling during this process. Furthermore, YAP1 together with miR-375 established a negative feedback loop to regulate osteogenesis. These findings suggest that miR-375 can be targeted to enhance bone formation and the feasibility of miRNA-targeted therapeutic approaches in bone tissue engineering.

EXPERIMENTAL PROCEDURES

Cell Culture and Osteogenic Induction

Primary hASCs from three different healthy human donors were obtained from ScienCell. Cells between three and five passages were used for the in vitro and in vivo experiments, and all the in vitro experiments were repeated in triplicate using hASCs from three donors, respectively. hASCs were cultured in PM containing DMEM with 10% (v/v) fetal bovine serum (FBS) and 1% (v/v) antibiotics at 37°C in an incubator with an atmosphere consisting of 95% air and 5% CO_2, with 100% relative humidity. For osteogenic differentiation, cells were cultured in OM, which consisted of DMEM with 10% (v/v) FBS, 1% (v/v) antibiotics, 100 nM dexamethasone, 10 mM β-glycerophosphate, and 0.2 mM L-ascorbic acid. 293T was obtained from the American Type Culture Collection and cultured in DMEM supplemented with 10% (v/v) FBS and 1% (v/v) antibiotics.

Lentivirus Infection

Lentivirus infection was performed as described previously (Fan et al., 2016). All recombinant lentiviruses were obtained from GenePharma and used for hASC infection at an MOI of 100. The packaged lentiviruses used contained pre-miR-375 (miR-375), NC, anti-sense miR-375 (anti-miR-375), and anti-sense NC (anti-NC). Infection was performed by exposing hASCs to dilutions of the viral supernatant in the presence of polybrene (5 μg/mL) and fresh medium for 24 hr, followed by selection with puromycin

(Sigma-Aldrich) at 1 μg/mL. Transduction efficiency was evaluated by determining the percentage of GFP-positive cells observed under an inverted fluorescence microscope (TE2000-U, Nikon).

RNA Interference and Transient Infection

Small interfering RNAs (siRNAs) targeting *DEPTOR*, *YAP1*, and NC were purchased from GenePharma. The sequences are listed in Table S2. For transient infection, cells were cultured and grown to 70%–90% confluence, then transfected with siRNAs using Lipofectamine 2000 (Invitrogen) according to the manufacturer's procedure. After 48 hr, cells were harvested for RNA and protein analyses. For osteogenic differentiation, cells were cultured in OM and harvested after 7 and 14 days.

Alkaline Phosphatase Staining and Quantification

Cells cultured in PM or OM for 7 days were assayed for ALP staining and activity. ALP staining was performed using an NBT/BCIP staining kit (CoWin Biotech) with nitroblue tetrazolium (NBT) and 5-bromo-4-chloro-3-indolyl phosphate (BCIP). ALP quantification was measured using an ALP assay kit (Nanjing Jiancheng Bioengineering Institute). The total protein content was determined in the same sample by the BCA method using a Pierce Protein Assay Kit (Thermo Fisher Scientific). ALP activity relative to the control treatment was calculated after normalization to the total protein content.

Alizarin Red S Staining and Quantification

Cells cultured in PM or OM for 14 days were assayed for ARS staining and quantification. Cultured cells were fixed in 4% paraformaldehyde and then stained with 1% ARS (pH 4.2; Sigma-Aldrich) for 20 min at room temperature. For quantitative assessment of the degree of mineralization, the stain was dissolved with 100 mM cetylpyridinium chloride (Sigma-Aldrich) for 1 hr and quantified by spectrophotometric absorbance at 570 nm. ARS intensity relative to the control treatment was calculated after normalization to the total protein content.

Von Kossa Staining

Cells cultured in PM or OM for 21 days were assayed using the VK staining method as described previously (Jin et al., 2016). In brief, cells were fixed with 4% paraformaldehyde for 30 min at room temperature and then incubated with 5% silver nitrate solution for 1 hr by exposure to a 50-W UV lamp. Unincorporated silver nitrate was removed using 5% sodium thiosulfate and rinsed three times with distilled water.

RNA Extraction, Reverse Transcription, and Real-Time qPCR

Total cellular RNAs were isolated on 7 and 14 days after osteoinduction using TRIzol reagent (Invitrogen) and used for first-strand cDNA synthesis with a Reverse Transcription System (Takara Bio). Quantification of all gene transcripts was performed by real-time qPCR using a Power SYBR Green PCR Master Mix (Roche) and a 7500 Real-Time PCR Detection System (Applied Biosystems). The following thermal settings were used: 95°C for 10 min, followed by 40 cycles of 95°C for 15 s and 60°C for 1 min. The internal controls for mRNAs and miR-375 were *GAPDH* and U6, respectively. The primers used are listed in Table S2. The data were analyzed using the $2^{-\Delta\Delta Ct}$ relative expression method.

Immunofluorescence Staining

Lentivirus-infected hASCs were seeded in 24-well plates. After 14 days of osteoinduction, cells grown on sterile glass coverslips were fixed in 4% paraformaldehyde for 30 min, permeabilized with 0.1% Triton X-100 for 15 min, and blocked with 5% normal goat serum for 30 min. Thereafter, cells were incubated with a primary antibody (1:200) against osteocalcin (OCN; Abcam) overnight at 4°C, then incubated in the presence of an anti-mouse secondary antibody (1:500; Cell Signaling Technology) for 1 hr at room temperature. Nuclei were counterstained with 4′,6-diamidino-2-phenylindole (DAPI), and the coverslips were mounted on a glass slides and viewed under a Confocal Zeiss Axiovert 650 microscope at wavelengths of 488 nm (green, OCN) and 405 nm (blue, DAPI). Images were captured using an LSM 5 Exciter confocal imaging system (Carl Zeiss).

Western Blot Analysis

After 7 and 14 days of osteoinduction, infected hASCs were harvested, washed with PBS, and lysed in RIPA buffer containing 1% PMSF (Sigma-Aldrich). For mechanistic evaluation of miR-375, total proteins were extracted after 7 days of osteoinduction. For evaluation of osteogenesis, total proteins were extracted after 14 days of osteoinduction. Primary antibodies against RUNX2, DEPTOR, p-S6K (Thr389), p-mTOR (Ser2448), mTOR, p-AKT (Ser473), AKT, p-IRS1 (Ser636/639), and YAP1 (Cell Signaling Technology), and OCN and GAPDH (Abcam) were diluted 1:1,000 and incubated with the membranes at 4°C overnight. Horseradish peroxidase-conjugated anti-rabbit or anti-mouse secondary antibodies (Cell Signaling) were diluted 1:10,000 and incubated with the membranes at room temperature for 1 hr. The membranes were then visualized using an ECL kit (CWBIO). Band intensities were quantified using ImageJ software (https://imagej.nih.gov/ij/). The background was subtracted, and the signal of each target band was normalized to that of the GAPDH band.

Reporter Vector Construction

Reporter vectors were constructed by Integrated Biotech Solutions. In brief, the 3′ UTRs of *DEPTOR* and *YAP1* containing the predicted miR-375 binding sites were synthesized and cloned into a modified version of pcDNA3.1(+) that contained a firefly luciferase reporter gene (a gift from Professor Brigid L.M. Hogan, Duke University), at a position downstream of the luciferase reporter gene. Site-directed mutagenesis of selected putative seeding-sequence regions was performed using a Site-Directed Mutagenesis Kit (SBS Genetech). All constructs were confirmed by DNA sequencing.

Promoter Construction

Putative promoter of human miR-375 was amplified from the genomic DNA of HeLa cells and cloned into the PGL3-Enhancer vector (Promega). The primers for cloning the wild-type miR-375 promoter were as follows: sense, 5′-GGT GCC GTA CTT CCG CCA ATT-3′ and anti-sense, 5′-TCG CCC TCG GTG ATC TCC TG-3′.

Site-directed mutagenesis of YAP1-TEAD binding site on the miR-375 promoter was performed using a Site-Directed Mutagenesis Kit (SBS Genetech). The luciferase reporter plasmids containing the wild-type miR-375 promoter and the mutation of YAP1 binding site (−1,692/−1,687 bp) on the miR-375 promoter were constructed as above. All constructs were confirmed by DNA sequencing.

Dual-Luciferase Reporter Assay

Luciferase reporter assays were performed as described previously (Jia et al., 2014). In brief, 293T cells were grown in a 48-well plate and co-transfected with 400 ng of either control plasmid or plasmid-expressing targeting gene, 40 ng of the firefly luciferase reporter plasmid, and 4 ng of pRL-TK, a plasmid-expressing Renilla luciferase (Promega). Renilla and firefly luciferase activities were measured 24 hr after transfection using the Dual-Luciferase Reporter Assay System (Promega). All luciferase values were normalized to those of Renilla luciferase and expressed as fold induction relative to the basal activity.

Chromatin Immunoprecipitation Assay

ChIP assays were performed using an EZ-Magna ChIP assay kit (Merck Millipore) according to the manufacturer's instructions. hASCs were seeded in 10-cm dishes and transfected with *YAP1* siRNA or the NC. After 48 hr, cells were crosslinked with 1% formaldehyde, collected, lysed, and sonicated to shear DNA. Then the DNA-protein complexes were isolated with antibodies against isotype immunoglobulin G (IgG) and YAP1 (Cell Signaling). The protein-DNA complexes were then eluted and reverse-crosslinked. Spin columns were used to purify the DNA, which was quantified by qRT-PCR. Relative enrichment was calculated as the amount of amplified DNA normalized to the input and relative to values obtained from immunoprecipitation using normal IgG. The primers used are listed in Table S2.

Microarray and Bioinformatics

After 7 days of osteoinduction, total RNA was isolated from hASCs transfected with miR-375 and NC. Biotinylated cDNA was prepared according to the standard Affymetrix protocol from 250 ng of total RNA by using the Ambion WT Expression Kit (Thermo Fisher Scientific). Following labeling, 5.5 μg of cDNA was hybridized for 16 hr at 45°C on a GeneChip Human Transcriptome Array 2.0. GeneChips were washed and stained in the Affymetrix Fluidics Station 450. GeneChips were scanned by using the Affymetrix GeneChip Command Console (GPL15207, CapitalBio) installed in a GeneChip Scanner 3000 7G. Data were analyzed using the robust multichip analysis (RMA) algorithm with the Affymetrix default analysis settings. Values presented are $\log_2$ RMA signal intensities. For the calling of differentially expressed genes, the fold differences ($\geq$1.5 and $\leq$0.667), false discovery rate (<0.001), and average expression were used. For the gene ontology enrichment and KEGG pathway analysis, the DAVID webserver (http://david.ncifcrf.gov/) was used.

In Vivo Implantation of hASCs and SynthoGraft Hybrids

hASCs at the fourth passage infected with lentivirus (miR-375 or NC) were cultured in OM for 7 days prior to the in vivo study. After being trypsinized and resuspended directly in DMEM, the cells were incubated with synthograft (β-tricalcium phosphate; Bicon) for 1 hr at 37°C, followed by centrifugation at 150 × *g* for 5 min, then implanted into two symmetrical sites on the dorsal subcutaneous space of 6-week-old BALB/c homozygous nude (nu/nu) mice (n = 6 per group). This study was approved by the Institutional Animal Care and Use Committee of the Peking University Health Science Center (LA2014233), and all animal experiments were performed in accordance with the Institutional Animal Guidelines.

Analyses of Bone Formation In Vivo

Specimens were harvested 8 weeks after implantation, and the animals were euthanized by CO_2 asphyxiation. After fixation in 4% paraformaldehyde, the specimens were analyzed by high-resolution Inveon micro-CT (Siemens). In brief, an X-ray voltage of 80 kV, a node current of 500 μA, and an exposure time of 500 ms for each of the 360 rotational steps were used. For quantitative analysis of the images, the BV/TV) and BS/TV ratios were calculated using the Inveon Research Workplace software. The specimens were then decalcified in 10% EDTA (pH 7.4) for 14 days, followed by dehydration and embedding with paraffin. Sections (5 μm thickness) were cut and stained with H&E and Masson's trichrome. Immunohistochemical staining was performed with a primary antibody against OCN (Abcam) to investigate osteogenesis. Tissue slices were visualized under a light microscope (Olympus).

Statistical Analysis

Statistical analysis was performed using the SPSS Statistics 20.0 software (IBM). Data are expressed as mean ± SD of three independent experiments. Differences between two groups were analyzed by a Student's t test. For the testing of multiple groups, a one-way ANOVA was conducted. A two-tailed p value of <0.05 was considered to indicate statistical significance.

ACCESSION NUMBERS

All the raw and processed microarray data were deposited in the GEO database at the National Center for Biotechnology Information, and can be accessed by the accession number GEO: GSE87160.

SUPPLEMENTAL INFORMATION

Supplemental Information includes five figures and two tables and can be found with this article online at http://dx.doi.org/10.1016/j.stemcr.2017.01.028.

AUTHOR CONTRIBUTIONS

C.S., L.J., and Y. Zhou. designed and conducted experiments, collected and analyzed data, and wrote the manuscript. Y. Zheng and S.Z. assisted in carrying out experiments. Y. Zheng assisted in data analysis. Y. Zhou approved the final manuscript.

ACKNOWLEDGMENTS

This study was financially supported by grants from the National Natural Science Foundation of China (81371118, 81402235), the Culturing Program for Leading Talents in Beijing Science and

Technology Innovation (Lj201725), the Ph.D. Programs Foundation of Ministry of Education of China (20130001110101), and the foundation of the Peking University School and Hospital of Stomatology (PKUSS20140104).

Received: October 20, 2016
Revised: January 24, 2017
Accepted: January 26, 2017
Published: March 2, 2017

REFERENCES

Agrawal, P., Reynolds, J., Chew, S., Lamba, D.A., and Hughes, R.E. (2014). DEPTOR is a stemness factor that regulates pluripotency of embryonic stem cells. J. Biol. Chem. *289*, 31818–31826.

Biton, M., Levin, A., Slyper, M., Alkalay, I., Horwitz, E., Mor, H., Kredo-Russo, S., Avnit-Sagi, T., Cojocaru, G., Zreik, F., et al. (2011). Epithelial microRNAs regulate gut mucosal immunity via epithelium—T cell crosstalk. Nat. Immunol. *12*, 239–246.

Bosnakovski, D., Mizuno, M., Kim, G., Takagi, S., Okumura, M., and Fujinaga, T. (2005). Isolation and multilineage differentiation of bovine bone marrow mesenchymal stem cells. Cell Tissue Res. *319*, 243–253.

Caron, A., Labbe, S.M., Lanfray, D., Blanchard, P.G., Villot, R., Roy, C., Sabatini, D.M., Richard, D., and Laplante, M. (2016). Mediobasal hypothalamic overexpression of DEPTOR protects against high-fat diet-induced obesity. Mol. Metab. *5*, 102–112.

Chaulk, S.G., Lattanzi, V.J., Hiemer, S.E., Fahlman, R.P., and Varelas, X. (2014). The Hippo pathway effectors TAZ/YAP regulate dicer expression and microRNA biogenesis through Let-7. J. Biol. Chem. *289*, 1886–1891.

Deng, Y., Zhou, H., Zou, D., Xie, Q., Bi, X., Gu, P., and Fan, X. (2013). The role of miR-31-modified adipose tissue-derived stem cells in repairing rat critical-sized calvarial defects. Biomaterials *34*, 6717–6728.

Dibble, C.C., and Cantley, L.C. (2015). Regulation of mTORC1 by PI3K signaling. Trends Cell Biol. *25*, 545–555.

Ding, L., Xu, Y., Zhang, W., Deng, Y., Si, M., Du, Y., Yao, H., Liu, X., Ke, Y., Si, J., et al. (2010). MiR-375 frequently downregulated in gastric cancer inhibits cell proliferation by targeting JAK2. Cell Res. *20*, 784–793.

Du, F., Wu, H., Zhou, Z., and Liu, Y.U. (2015). microRNA-375 inhibits osteogenic differentiation by targeting runt-related transcription factor 2. Exp. Ther. Med. *10*, 207–212.

EI Ouaamari, A., Baroukh, N., Martens, G.A., Lebrun, P., Pipeleers, D., and van Obberghen, E. (2008). miR-375 targets 3′-phosphoinositide-dependent protein kinase-1 and regulates glucose-induced biological responses in pancreatic beta-cells. Diabetes *57*, 2708–2717.

Fan, C., Jia, L., Zheng, Y., Jin, C., Liu, Y., Liu, H., and Zhou, Y. (2016). MiR-34a promotes osteogenic differentiation of human adipose-derived stem cells via the RBP2/NOTCH1/CYCLIN D1 coregulatory network. Stem Cell Rep. *7*, 236–248.

Fang, S., Deng, Y., Gu, P., and Fan, X. (2015). MicroRNAs regulate bone development and regeneration. Int. J. Mol. Sci. *16*, 8227–8253.

Farazi, T.A., Hoell, J.I., Morozov, P., and Tuschl, T. (2013). MicroRNAs in human cancer. Adv. Exp. Med. Biol. *774*, 1–20.

Guan, M., Yao, W., Liu, R., Lam, K.S., Nolta, J., Jia, J., Panganiban, B., Meng, L., Zhou, P., Shahnazari, M., et al. (2012). Directing mesenchymal stem cells to bone to augment bone formation and increase bone mass. Nat. Med. *18*, 456–462.

Ha, M., and Kim, V.N. (2014). Regulation of microRNA biogenesis. Nat. Rev. Mol. Cell Biol. *15*, 509–524.

Hansen, C.G., Moroishi, T., and Guan, K.L. (2015a). YAP and TAZ: a nexus for Hippo signaling and beyond. Trends Cell Biol. *25*, 499–513.

Hansen, C.G., Ng, Y.L., Lam, W.L., Plouffe, S.W., and Guan, K.L. (2015b). The Hippo pathway effectors YAP and TAZ promote cell growth by modulating amino acid signaling to mTORC1. Cell Res. *25*, 1299–1313.

Hilton, C., Neville, M.J., and Karpe, F. (2013). MicroRNAs in adipose tissue: their role in adipogenesis and obesity. Int. J. Obes. (Lond) *37*, 325–332.

Hong, W., and Guan, K.L. (2012). The YAP and TAZ transcription co-activators: key downstream effectors of the mammalian Hippo pathway. Semin. Cell Dev. Biol. *23*, 785–793.

Hong, J.H., Hwang, E.S., McManus, M.T., Amsterdam, A., Tian, Y., Kalmukova, R., Mueller, E., Benjamin, T., Spiefelman, B.M., Sharp, P.A., et al. (2005). TAZ, a transcriptional modulator of mesenchymal stem cell differentiation. Science *309*, 1074–1078.

Jia, L.F., Huang, Y.P., Zheng, Y.F., Lyn, M.Y., Wei, S.B., Meng, Z., and Gan, Y.H. (2014). miR-29b suppresses proliferation, migration, and invasion of tongue squamous cell carcinoma through PTEN-AKT signaling pathway by targeting Sp1. Oral Oncol. *50*, 1062–1071.

Jin, C., Jia, L., Huang, Y., Zheng, Y., Du, N., Liu, Y., and Zhou, Y. (2016). Inhibition of lncRNA MIR31HG promotes osteogenic differentiation of human adipose-derived stem cells. Stem Cells http://dx.doi.org/10.1002/stem.2439.

Kim, Y.J., Bae, S.W., Yu, S.S., Bae, Y.C., and Jung, J.S. (2009). miR-196a regulates proliferation and osteogenic differentiation in mesenchymal stem cells derived from human adipose tissue. J. Bone Miner. Res. *24*, 816–825.

Kim, M., Kim, T., Johnson, R.L., and Lim, D.S. (2015). Transcriptional co-repressor function of the hippo pathway transducers YAP and TAZ. Cell Rep. *11*, 270–282.

Laplante, M., and Sabatini, D.M. (2012). mTOR signaling in growth control and disease. Cell *149*, 274–293.

Laplante, M., Horvat, S., Festuccia, W.T., Birsoy, K., Prevorsek, Z., Efeyan, A., and Sabatini, D.M. (2012). DEPTOR cell-autonomously promotes adipogenesis, and its expression is associated with obesity. Cell Metab. *16*, 202–212.

Lian, I., Kim, J., Okazawa, H., Zhao, J., Zhao, B., Yu, J., Chinnaiyan, A., Israel, M.A., Goldstein, L.S., Abujarour, R., et al. (2010). The role of YAP transcription coactivator in regulating stem cell self-renewal and differentiation. Genes Dev. *24*, 1106–1118.

Liu, A.M., Poon, R.T., and Luk, J.M. (2010). MicroRNA-375 targets Hippo-signaling effector YAP in liver cancer and inhibits tumor properties. Biochem. Biophys. Res. Commun. *394*, 623–627.

Liu, S., Sun, G., Yuan, B., Zhang, L., Gao, Y., Jiang, H., Dai, L., and Zhang, J. (2016a). miR-375 negatively regulates porcine preadipocyte differentiation by targeting BMPR2. FEBS. Lett. *590*, 1417–1427.

Martin, S.K., Fitter, S., Bong, L.F., Drew, J.J., Gronthos, S., Shepherd, P.R., and Zannettino, A.C. (2010). NVP-BEZ235, a dual pan class I PI3 kinase and mTOR inhibitor, promotes osteogenic differentiation in human mesenchymal stromal cells. J. Bone Miner. Res. *25*, 2126–2137.

Martin, S.K., Fitter, S., Dutta, A.K., Matthews, M.P., Walkley, C.R., Hall, M.N., Ruegg, M.A., Gronthos, S., and Zannettino, A.C. (2015). Brief report: the differential roles of mTORC1 and mTORC2 in mesenchymal stem cell differentiation. Stem Cells *33*, 1359–1365.

Meng, Z., Moroishi, T., and Guan, K.L. (2016). Mechanisms of Hippo pathway regulation. Genes Dev. *30*, 1–17.

Mori, M., Triboulet, R., Mohseni, M., Schlegelmilch, K., Shrestha, K., Camorgo, F.D., and Gregory, R.I. (2014). Hippo signaling regulated microprocessor and links cell-density-dependent miRNA biogenesis to cancer. Cell *156*, 893–906.

Novack, D.V. (2011). Role of NF-κB in the skeleton. Cell Res. *21*, 169–182.

Peterson, T.R., Laplante, M., Thoreen, C.C., Sancak, Y., Kang, S.A., Kuehi, W.M., Gray, N.S., and Sabatini, D.M. (2009). DEPTOR is an mTOR inhibitor frequently overexpressed in multiple myeloma cells and required for their survival. Cell *137*, 873–886.

Petite, H., Viateau, V., Bensaid, W., Meunier, A., Pollak, C., Bourguignon, M., Oudina, K., Sedel, L., and Guillemin, G. (2000). Tissue-engineered bone regeneration. Nat. Biotechnol. *18*, 959–963.

Poy, M.N., Eliasson, L., Krutzfeldt, J., Kuwajima, S., Ma, X., Macdonald, P.E., Pfeffer, S., Tuschil, T., Rajewsky, N., Rorsman, P., et al. (2004). A pancreatic islet-specific microRNA regulates insulin secretion. Nature *432*, 226–230.

Salazar, V.S., Gamer, L.W., and Rosen, V. (2016). BMP signaling in skeletal development, disease and repair. Nat. Rev. Endocrinol. *12*, 203–221.

Selth, L.A., Das, R., Townley, S.L., Coutinho, I., Hanson, A.R., Centenera, M.M., Stylianou, N., Sweeney, K., Soekmadji, C., Jovanovic, L., et al. (2016). A ZEB1-miR-375-YAP1 pathway regulates epithelial plasticity in prostate cancer. Oncogene *36*, 24–34.

Sen, B., Xie, Z., Uzer, G., Thompson, W.R., Styner, M., Wu, X., and Rubin, J. (2015). Intranuclear actin regulates osteogenesis. Stem Cells *33*, 3065–3076.

Seo, E., Basu-Roy, U., Gunaratne, P.H., Coarfa, C., Lim, D.S., Basilico, C., and Mansukhani, A. (2013). SOX2 regulates YAP1 to maintain stemness and determine cell fate in the osteo-adipo lineage. Cell Rep. *3*, 2075–2087.

Shimobayashi, M., and Hall, M.N. (2014). Making new contacts: the mTOR network in metabolism and signaling crosstalk. Nat. Rev. Mol. Cell Biol. *15*, 155–162.

Srinivas, K.P., Viji, R., Dan, V.M., Sajitha, I.S., Prakash, R., Rahul, P.V., Santhoshkumar, T.R., Lakshmi, S., and Pillai, M.R. (2016). DEPTOR promotes survival of cervical squamous cell carcinoma cells and its silencing induces apoptosis through down- regulating PI3K/AKT and by up-regulating p38 MAP kinase. Oncotarget *7*, 24154–24171.

Sun, Y., Xu, L., Huang, S., Hou, Y., Liu, Y., Chan, K.M., Pan, X.H., and Li, G. (2015). mir-21 overexpressing mesenchymal stem cells accelerate fracture healing in a rat closed femur fracture model. Biomed. Res. Int. *2015*, 412327.

Takada, I., Kouzmenko, A.P., and Kato, S. (2009). Wnt and PPARgamma signaling in osteoblastgenesis and adipogenesis. Nat. Rev. Rheumatol. *5*, 442–447.

Tumaneng, K., Schlegelmilch, K., Russell, R.C., Yimlamai, D., Basnet, H., Mahadevan, N., Fitamant, J., Bardeesy, N., Camargo, F.D., and Guan, K.L. (2012). YAP mediates crosstalk between the Hippo and PI3K-TOR pathways by suppressing PTEN via miR-29. Nat. Cell Biol. *14*, 1322–1329.

Verma, S., Rajaratnam, J.H., Denton, J., Hoyland, J.A., and Byers, R.J. (2002). Adipocytic proportion of bone marrow is inversely related to bone formation in osteoporosis. J. Clin. Pathol. *55*, 693–698.

Xi, J.C., Zang, H.Y., Guo, L.X., Xue, H.B., Liu, X.D., Bai, Y.B., and Ma, Y.Z. (2015). The PI3K/AKT cell signaling pathway is involved in regulation of osteoporosis. J. Recept. Signal. Transduct. Res. *35*, 640–645.

Yan, J.W., Lin, J.S., and He, X.X. (2014). The emerging role of miR-375 in cancer. Int. J. Cancer *135*, 1011–1018.

Yang, C., Tibbitt, M.W., Basta, L., and Anseth, K.S. (2014). Mechanical memory and dosing influence stem cell fate. Nat. Mater. *13*, 645–652.

Zhang, Z.W., Men, T., Feng, R.C., Li, Y.C., Zhou, D., and Teng, C.B. (2013). miR-375 inhibits proliferation of mouse pancreatic progenitor cells by targeting YAP1. Cell Physiol. Biochem. *32*, 1808–1817.

Zhang, X., Li, Y., Chen, Y.E., Chen, J., and Ma, P.X. (2016). Cell-free 3D scaffold with two-stage delivery of miRNA-26a to regenerate critical-sized bone defects. Nat. Commun. *7*, 10376.

Zhao, B., Tumaneng, K., and Guan, K.L. (2011). The Hippo pathway in organ size control, tissue regeneration and stem cell self-renewal. Nat. Cell Biol. *13*, 877–883.

Zhou, J., Song, S., He, S., Zhu, X., Zhang, Y., Yi, B., Zhang, B., Qin, G., and Li, D. (2014). MicroRNA-375 targets PDK1 in pancreatic carcinoma and suppresses cell growth through the Akt signaling pathway. Int. J. Mol. Med. *33*, 950–956.

Zuk, P.A., Zhu, M., Ashjian, P., De Ugarte, D.A., Huang, J.I., Mizuno, H., Alfonso, Z.C., Fraser, J.K., Benhaim, P., and Hedrick, M.H. (2002). Human adipose tissue is a source of multipotent stem cells. Mol. Biol. Cell *13*, 4279–4295.

Stem Cell Reports, Volume *8*

Supplemental Information

Promotion Effects of miR-375 on the Osteogenic Differentiation of Human Adipose-Derived Mesenchymal Stem Cells

Si Chen, Yunfei Zheng, Shan Zhang, Lingfei Jia, and Yongsheng Zhou

Supplemental Figures:

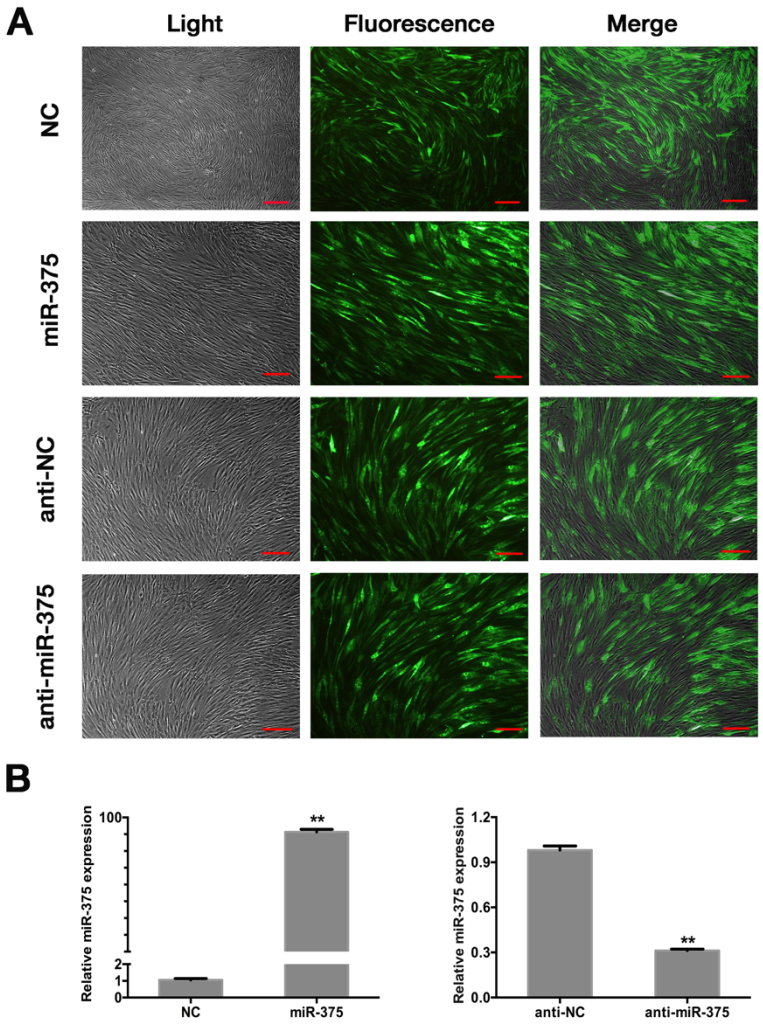

Figure S1 (related to main figure 2). Transduction efficiency of lentivirus containing miR-375, anti-miR-375, or control vectors. (A) Micrographs of GFP-positive hASCs under ordinary and fluorescent light. Scale bars: 500 μm. (B) Left: relative miR-375 expression in miR-375 and NC groups as determined by qRT-PCR. Right: relative miR-375 expression in anti-miR-375 and anti-NC groups as determined by qRT-PCR. U6 was used for normalization. Data are represented as mean ± SD; *$p < 0.05$, **$p < 0.01$ ($n = 3$ independent experiments).

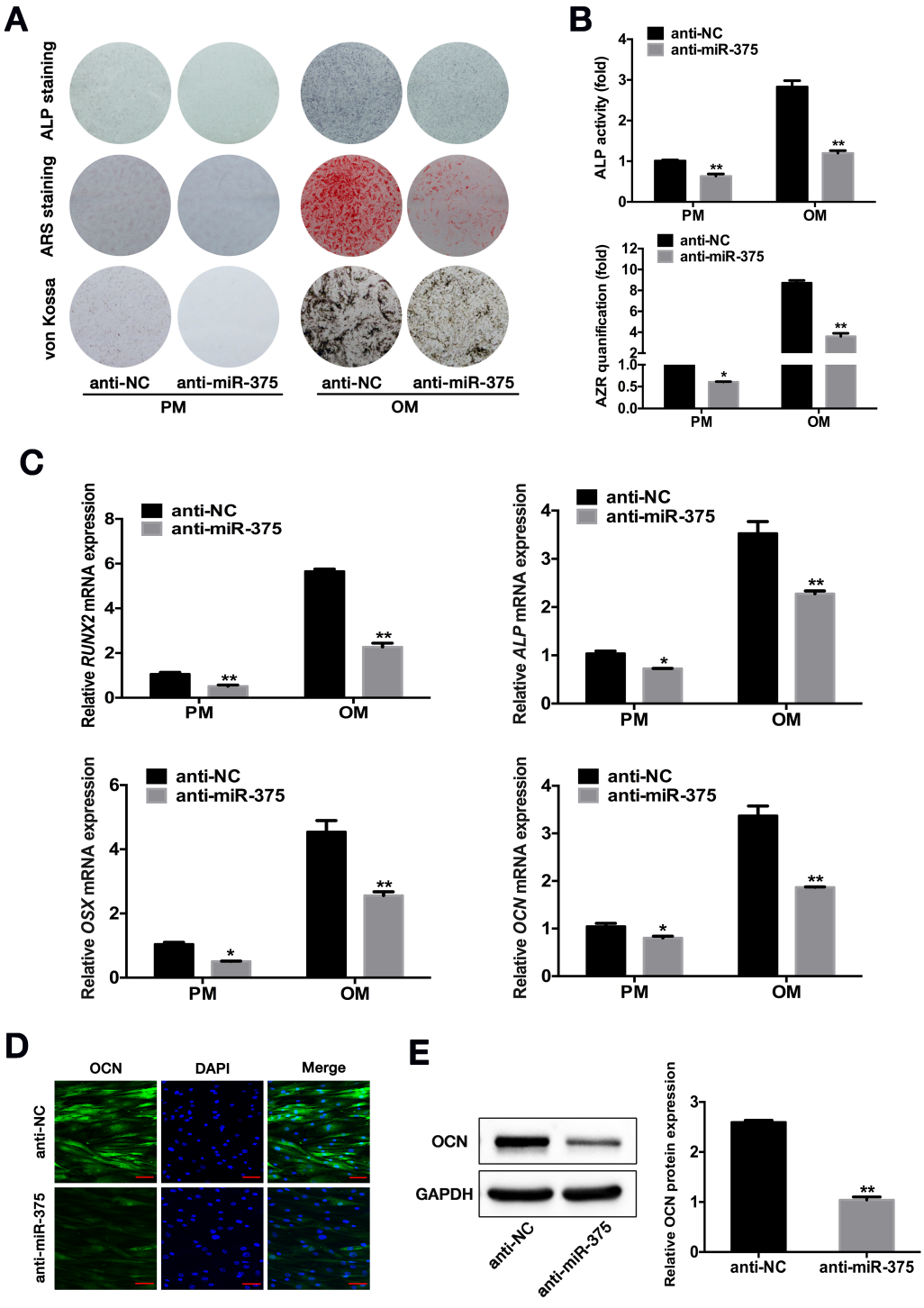

Figure S2 (related to main figure 2). miR-375 knockdown inhibits the osteogenic differentiation of hASCs. hASCs were transfected with lentivirus expressing anti-miR-375 or control vector (anti-NC), and cultured in proliferation medium (PM) or osteogenic medium (OM). (A) Alkaline phosphatase (ALP) staining on day 7, Alizarin Red S (ARS) staining on day 14, and von Kossa (VK) staining on day 21 after osteogenic induction. (B) ALP activity on day 7 and ARS mineralization assay on day 14 after osteogenic induction. (C) Relative mRNA levels of *RUNX2* and *ALP* measured by qRT-PCR on day 7 of osteogenic induction. Relative mRNA levels of *OSX* and *OCN* measured by qRT-PCR on day 14 of osteogenic induction. *GAPDH* was used for normalization. (D) Confocal microscopy of OCN with DAPI counterstaining on day 14 after osteogenic induction. Scale bars:

200 μm. (E) Left: western blot of OCN protein level on day 14 after osteogenic induction. GAPDH was used as the internal control. Right: quantification of band intensities. Data are represented as mean ± SD; *p < 0.05, **p < 0.01 (n = 3 independent experiments).

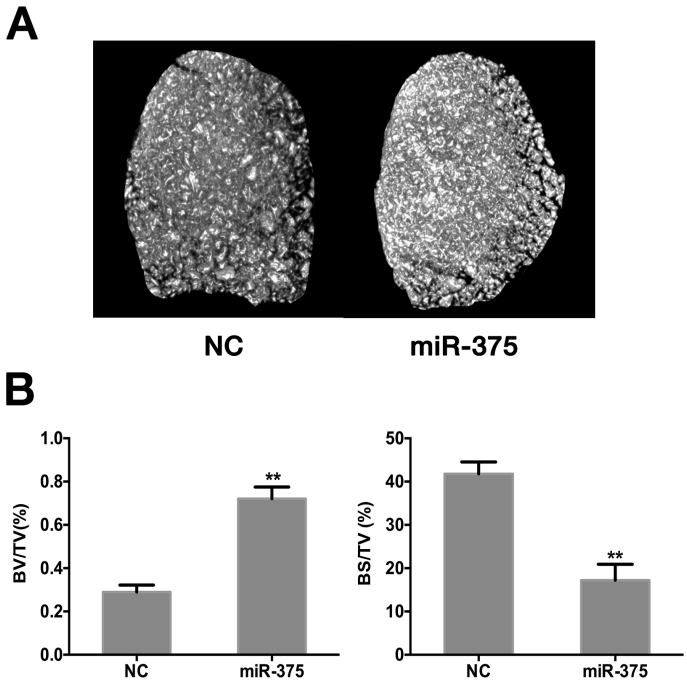

Figure S3 (related to main figure 3). miR-375 overexpression promotes heterotopic bone formation in vivo. (A) Representative micro-CT images of bone formation in miR-375 and NC groups. (B) Quantitative analysis of bone volume/tissue volume (BV/TV) and bone surface/tissue volume (BS/TV) in miR-375 and NC groups. Data are represented as mean ± SD; *p < 0.05, **p < 0.01 (n = 3 independent experiments).

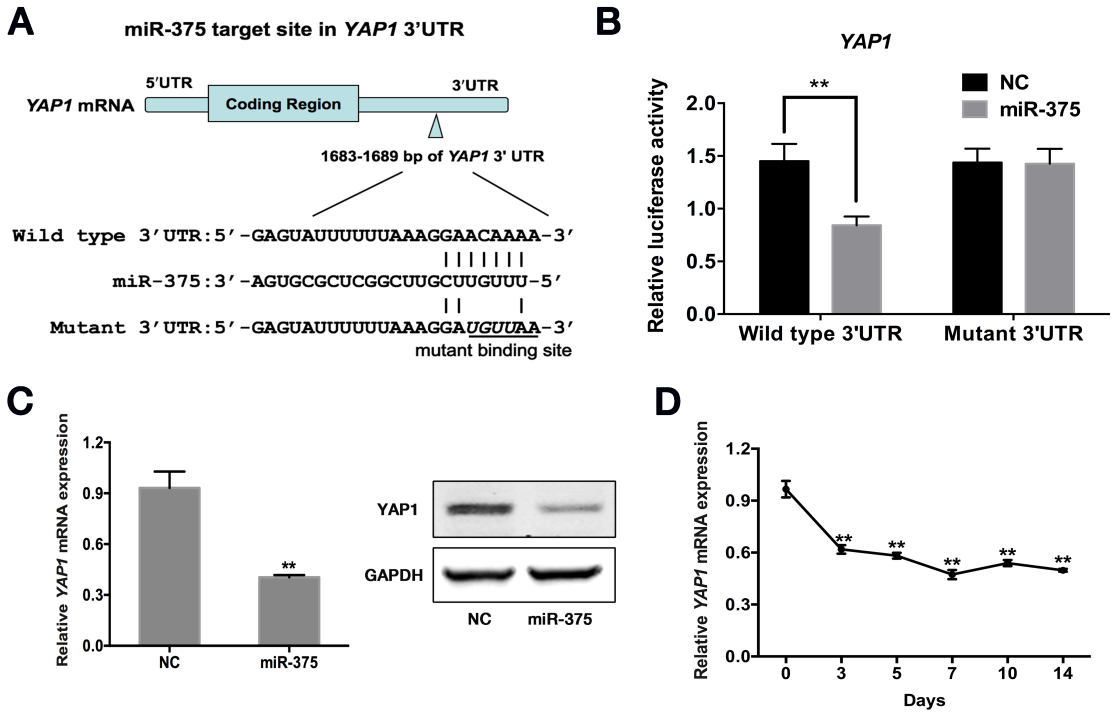

1) Figure S4 (related to main figure 7). miR-375 suppresses *YAP1* via directly targeting its 3'UTR. (A) Binding site of miR-375 in the 3'UTR of *YAP1*-WT mRNA (mutated bases in the 3'UTR of *YAP1*-MT are underlined). (B) Luciferase activity of cells with miR-375 overexpression in the *YAP1*-WT or *YAP1*-MT groups. (C) Relative mRNA and protein levels of YAP1 in miR-375 and NC groups as determined by qRT-PCR and western blot. GAPDH was used for normalization and the internal control. (D) Relative mRNA levels of *YAP1* at various time points during the osteogenic differentiation of hASCs as determined by qRT-PCR. *GAPDH* was used for normalization. Data are represented as mean ± SD; *p < 0.05, **p < 0.01 (n = 3 independent experiments).

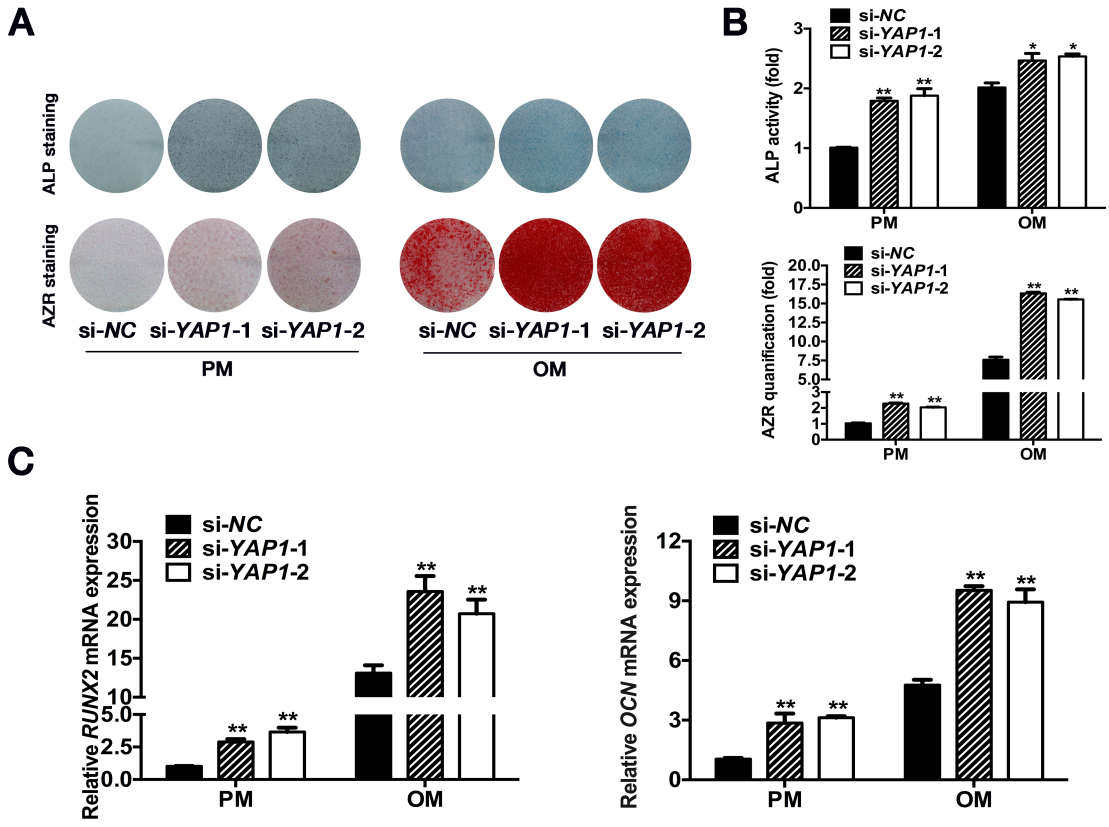

Figure S5 (related to main figure 7). Knockdown of *YAP1* enhanced the osteogenic differentiation of hASCs. (A) Alkaline phosphatase (ALP) staining on day 7 and Alizarin Red S (ARS) staining on day 14 after osteogenic induction. (B) ALP activity on day 7 and ARS mineralization assay on day 14 after osteogenic induction. (C) Relative mRNA levels of *RUNX2* and *OCN* as determined by qRT-PCR on day 14 of osteogenic induction. *GAPDH* was used for normalization. Data are represented as mean ± SD; *p < 0.05, **p < 0.01 (n = 3 independent experiments).

Supplemental Tables

Table S1. Gene expression in the osteogenic differentiation of hASCs transfected with miR-375 by microarray analysis ($p < 0.001$).

Upregulation		Downregulation	
Gene Name	Fold Change	Gene Name	Fold Change
MMP1	8.0583	***DEPTOR***	**0.3794**
MMP3	5.8323	*ERG1*	0.399
COL10AQ	3.633	*MGARP*	0.404
PARRES2	2.6751	*CTSC*	0.4061
ADRA2A	2.5316	*MEST*	0.4194
CXCL5	2.391	*FRZB*	0.4449
COL10A1	2.2842	*INMT*	0.4455
AKR1C1	2.2155	*SERPINB2*	0.4468
CD163	2.1417	*FHL1*	0.4661
G0S2	2.0636	*HSPB7*	0.4697
		FAM43A	0.4709
		EFHD1	0.473
		KPTAP1-5	0.4809
		ELN	0.4836

Table 1 shows the fold changes of gene expression: ≥ 2 indicates upregulation and ≤ 0.5 indicates downregulation. ***DEPTOR*** decreased most among the downregulated genes with miR-375 overexpression in hASCs.

Table S2. Sequences of RNA and DNA oligonucleotides.

Name	Sense Strand/Sense Primer (5'-3')	Antisense Strand/Antisense Primer (5'-3')
siRNA		
*DEPTOR*1	GUCAUCAUCUCAAGACCUATT	UAGGUCUUGAGAUGAUGACTT
*DEPTOR*2	GUCUGUCAGUUUGUCGUCUTT	AGACGACAAACUGACAGACTT
YAP1-1	GGUGAUACUAUCAACCAAATT	UUUGGUUGAUAGUAUCACCTT
YAP1-2	GACGACCAAUAGCUCAGAUTT	AUCUGAGCUAUUGGUCGUCTT
NC	UUCUCCGAACGUGUCACGUTT	ACGUGACACGUUCGGAGAATT
Primers for qRT-PCR		
miR-375 RT primer	GCTGTCAACGATACGCTACCTAACGGCATGACAGTGTCAGCCTA	
miR-375	GTGCAGGGTCCGAGGT	AGCCGTTTGTTCGTTCGGCT
U6	CTCGCTTCGGCAGCACA	AACGCTTCACGAATTTGCGT
RUNX2	CCGCCTCAGTGATTTAGGGC	GGGTCTGTAATCTGACTCTGTCC
ALP	ATGGGATGGGTGTCTCCACA	CCACGAAGGGGAACTTGTC
OSX	CCTCTGCGGGACTCAACAAC	TAAAGGGGCTGGATAAGCAT
OCN	CACTCCTCGCCCTATTGGC	CCCTCCTGCTTGGACACAAAG
DEPTOR	TTTGTGGTGCGAGGAAGTAA	CATTGCTTTGTGTCATTCTGG
YAP1	ACCCTCGTTTTGCCATGAAC	TTGTTTCAACCGCAGTCTCTC
GAPDH	GAAGGTGAAGGTCGGAGTC	GAAGATGGTGATGGGATTTC
Primers for ChIP-qPCR		
Ch-1	CCAGTAGCACTACATTTGGGTTAA	CTGTGGCAGCCATGACATTC
Ch-2	CGTGGGCAACATAGCAAGAC	GCACCTCAGCCTCCAAAGTAA
Ch-3	GGTGCCGTACTTCCGCCAATT	CTCCTCCAACTCTTCTTCTTCCTCTTC
Ch-4	GTGGTGCCACTTCCTACCGA	CCCTGCCATCCTTCCCTCT
Ch-5	GGTCGAGGTCACCACTGGATT	AGGGAGGAGCCGAGAAGCA

Abbreviation: *DEPTOR*, dep-domain containing mTOR-interacting protein; *YAP1*, Yes-associated protein 1. *RUNX2*, runt-related transcription factor 2; *ALP*, alkaline phosphatase; *OSX*, osterix; *OCN*, osteocalcin.